SDC

OPEN

SIBLING CONCORDANCE IN SYMPTOM ONSET AND ATROPHY GROWTH RATES IN STARGARDT DISEASE USING ULTRA-WIDEFIELD FUNDUS AUTOFLUORESCENCE

RACHAEL C. HEATH JEFFERY, MChD, MPH,*† JENNIFER A. THOMPSON, PhD,‡ JOHNNY LO, PhD,§ TINA M. LAMEY, PhD,*‡ TERRI L. McLAREN, BSc,*‡ JOHN N. DE ROACH, PhD,*‡ DIMITAR N. AZAMANOV, MD, PhD,¶ IAN L. McALLISTER, MD,* IAN J. CONSTABLE, MD,* FRED K. CHEN, MBBS, PhD*†**

Purpose: To investigate concordance in symptom onset, area of dark autofluorescence (DAF), and growth rate (GR) between Stargardt disease siblings at an age-matched time point.

Methods: In this retrospective longitudinal study of sibling pairs with identical biallelic *ABCA4* variants, age at symptom onset, best-corrected visual acuity, atrophy area, and effective radius of DAF on ultra-widefield fundus autofluorescence were recorded. Absolute intersibling differences for both eyes were compared with absolute interocular differences using the Mann–Whitney test.

Results: Overall 39 patients from 19 families were recruited. In 16 families, age-matched best-corrected visual acuity and DAF were compared between siblings. In 8 families, DAF GR was compared. The median (range) absolute difference in age at symptom onset between siblings was 3 (0–35) years. Absolute intersibling differences in age-matched best-corrected visual acuity were greater than interocular differences ($P = 0.01$). Similarly, absolute intersibling differences in DAF area and radius were greater than interocular differences ($P = 0.04$ for area and $P = 0.001$ for radius). Differences between absolute interocular and intersibling GR were not statistically significant ($P = 0.44$ for area GR and $P = 0.61$ for radius GR).

Conclusion: There was significant discordance in age-matched best-corrected visual acuity and DAF beyond the expected limits of interocular asymmetry. Lack of significant intersibling differences in GR warrants further investigation.

RETINA 42:1545–1559, 2022

Stargardt disease (STGD1, OMIM #248200), caused by biallelic variants in the ATP-binding cassette transporter subfamily A4 (*ABCA4*) gene, is one of the most common inherited retinal diseases (IRDs)[1–4] and accounts for 12% of IRD-related blindness certification.[5] A significant proportion of STGD1 families have more than one affected family member. Despite carrying identical *ABCA4* variants, previous reports have shown that affected siblings may have significant discordance in their age at onset and disease severity.[6–8] Thus, a deeper understanding of the mechanisms behind sibling discordance is warranted for patient counselling and the identification of genetic modifiers.

An early description of 14 STGD1 families found sibling discordance in age at symptom onset and phenotype.[9] Lois et al[10] was the first to describe detailed intrafamilial phenotypic variation in 31 siblings from 15 families where a large difference in the age at symptom onset (median, 12 years; range, 5–23 years) was reported in 6 families despite similar electrodiagnostic findings. However, there were no data to confirm genetic concordance between these siblings. A retrospective cohort study by Valkenburg et al[11] evaluated 39 siblings from 17 families and found substantial differences (>10 years) in age at symptom onset in five families. When matched for disease duration, the area of central retinal pigment epithelial atrophy was highly comparable among 9 of these families (median, 11.38 and 10.59 mm^2 in the right and left eyes, respectively). However, they did not investigate intersibling

concordance in lesion growth rate nor did they use ultra-wide field (UWF) imaging to visualize lesions that extended beyond the central 30° field. Ultra-wide field-fundus autofluorescence (UWF-FAF) provides reliable quantification of the atrophy growth rate (GR).[12]

Given the paucity of data on intersibling concordance in disease onset and progression, we sought to evaluate the concordance in age at symptom onset, age-matched best-corrected visual acuity (BCVA), dark autofluorescence (DAF) area, and growth rates, as determined with UWF-FAF imaging, between siblings carrying identical *ABCA4* variants.

Methods

Study Design and Population

This longitudinal study collected retrospective and prospective data at the Lions Eye Institute, Perth, Australia, from June 2011 to November 2021. The study adhered to the tenets of the Declaration of Helsinki, and ethics approval was obtained from the Human Ethics Office of Research Enterprise, the University of Western Australia (RA/4/1/7916, 2021/ET000151). Informed consent was obtained from all participants.

All families with two or more siblings carrying identical *ABCA4* variants were eligible for inclusion. Siblings with only one variant or with two or more variants without evidence of biphasic status were excluded. Clinical data included age, sex, age at symptom onset, and BCVA as measured on the Early Treatment of Diabetic Retinopathy Study chart. Age-matched BCVA was collected for eligible sibling pairs in which assessment was performed at the same age (±1 year).

Imaging Procedures and Outcome Measures

Ultra-wide field-fundus autofluorescence images were obtained using the Optomap or California device (Optos PLC, Dunfermline, United Kingdom), elicited by a green excitation laser at 532nm.[19] Total retinal area was approximately 1081.6mm^2, and the maximum area imaged was 82.5%.[19] DAF was defined as a well-delineated confluent area of reduced autofluorescence similar in intensity to the hypoautofluorescent branching patterns created by the retinal vasculature blocking the retinal pigment epithelial autofluorescence signal. Speckled hypoautofluorescent regions surrounding an area of DAF were not included. Examples of DAF boundary segmentation are shown in **Supplemental Digital Content 1** (see **Supplementary Figure S1**, http://links.lww.com/IAE/B684). All images were manually outlined by two graders (R.C. H.J. & F.K.C.) using OptosAdvance software at baseline and the latest follow-up. The area in mm^2 was recorded. Dark autofluorescence attributed to masking by pigment plaques was excluded. Areas of DAF that extended outside the posterior pole were only included if they were contiguous with or within 3-disk diameters of the primary lesion. An age-matched DAF area was recorded for sibling pairs in which UWF-FAF imaging was performed at the same age (±1 year). We have previously demonstrated an interobserver limits of agreement of −3.13 to +2.87 mm^2 in DAF area (N = 61) and −0.20 to +0.17 mm square root area (N = 61) in patients with Stargardt disease using this technique.[12]

Electrodiagnostics were performed in keeping with the standards of the International Society for Clinical Electrophysiology of Vision (ISCEV) at the time of recording or our own in-house protocol before adoption of these standards.[13–16] Before 1999, an in-house, custom-built, full-field electroretinography (ERG) system used blue light for dim flash dark-adapted responses. From 1999 to 2012, the LKC UTAS E-3000 system (LKC Technologies, Inc, Gaithersburg) used 0.0068 cd.s.m^{-2} for the dim flash and 1.8 cd.s.m^{-2} as the standard flash. From 2012 full-field ERG incorporated

From the *Centre for Ophthalmology and Visual Science (incorporating Lions Eye Institute), The University of Western Australia, Australia; †Department of Ophthalmology, Royal Perth Hospital, Perth, Western Australia, Australia; ‡Australian Inherited Retinal Disease Registry and DNA Bank, Department of Medical Technology and Physics, Sir Charles Gairdner Hospital, Perth, Western Australia, Australia; §School of Science, Edith Cowan University, Perth, Western Australia, Australia; ¶Department of Diagnostic Genomics, PathWest, Perth, Western Australia, Australia; **Ophthalmology, Department of Surgery, University of Melbourne, Victoria, Australia; and ††Centre for Eye Research Australia, Royal Victorian Eye and Ear Hospital, Melbourne, Victoria, Australia.

Supported by the National Health & Medical Research Council of Australia (project and fellowship grant no.: GNT1116360 (F.K.C.), GNT1188694 (F.K.C.), GNT1054712 (F.K.C.) and MRF1142962 (F.K.C.)), the Perth Children's Hospital-Telethon research grant, Macular Disease Foundation Australia, the McCusker Charitable Foundation (F.K.C.), Miocevich Retina Fellowship (R.C.H.J.), and Retina Australia (J.A.T., T.L., J.N.D.R., T.L.M.).

None of the authors has any financial/conflicting interests to disclose.

Supplemental digital content is available for this article. Direct URL citations appear in the printed text and are provided in the HTML and PDF versions of this article on the journal's Web site (www.retinajournal.com).

Reprint requests: Fred K. Chen, MBBS, PhD, FRANZCO, Lions Eye Institute, 2 Verdun Street, Nedlands, 6009, WA, Australia; e-mail: fredchen@lei.org.au

the 2008 ISCEV update to include a dim (0.01 cd.s.m^{-2}), a standard (3.0 cd.s.m^{-2}), and a strong (10.0 cd.s.m^{-2}) white flash in a dark-adapted state to assess rod system function (RETIport 3.2, Roland Consult, Brandenburg, Germany). A 30 Hz and 2 Hz standard flash (3.0 cd.s.m^{-2}) were used in light-adapted condition to assess cone system function. The peak time (millisecond) and amplitude (microVolts) of all response components (a- and b-waves) were recorded and compared with internal normative data. Pattern ERG P50 and N95 amplitudes were used to assess macular function. Multifocal ERG (VERIS Science V6.3.2 system, Electro Diagnostic imaging Inc, San Mateo, CA) was performed using an array of 103 retinal-scaled hexagons covering 45° of visual angle to assess the topography of retinal dysfunction within the posterior pole. We classified patients into three groups.[17,18] Group 1 included those with a normal full-field ERG and abnormal pattern ERG consistent with macular dysfunction or reduced response densities within the central region of the multifocal ERG. Group 2 included those with generalized cone ERG abnormality as assessed with 2 Hz and 30 Hz standard flash in light adapted condition. Group 3 included those with generalized cone and rod ERG abnormalities as assessed with a dim, standard, and strong flash in dark-adapted condition.

Genetic Analysis

DNA was collected through the Australian Inherited Retinal Disease Registry and DNA Bank[19] or PathWest (local government pathology service). Genomic DNA was analyzed using disease-specific next-generation sequencing (NGS) SmartPanels[20] and whole-exome massive parallel sequencing. Candidate *ABCA4* mutations were confirmed in parents and other affected siblings by Sanger sequencing (genetic testing performed by CEI Molecular Diagnostics Laboratory (Portland, OR and PathWest, Australia). Variant nomenclature was described in relation to *ABCA4* coding DNA reference sequence NM_000350.2 and reported in accordance with the recommendations of the Human Genome Variation Society.[21] Pathogenicity was assessed as described previously[22] and interpreted according to the joint guidelines of the American College of Medical Genetics and Genomics and the Association for Molecular Pathology (ACMG/AMP)[23] and the associated literature.[24] Patients were classified into different genotypes, namely, Class A: biallelic null or severe variants, Class B: an intermediate variant in *trans* with another intermediate, null, or severe variant, and Class C: a mild or hypomorphic variant in *trans* with a null or severe variant.

Data and Statistical Analysis

Best-corrected visual acuity of counting fingers, hand motion, and perception of light were assigned −15, −30, and −45 letter scores, respectively, using the Freiburg test.[25,26]

Total DAF area and effective lesion radius growth rate (GR) were calculated.[27] Note in those patients with multifocal lesions, a theoretical effective radius was calculated based on the combined DAF area. Square root transformation of the measured combined DAF area was performed before the calculation of the effective lesion radius GR using the formula:

$$DAF\ \ Effective\ \ Radius\ \ GR(mm/year) = \frac{\left(\sqrt{\text{DAF final}} - \sqrt{\text{DAF baseline}}\right)}{\left(\sqrt{\pi}\right) \times \left(\text{Follow up duration (years)}\right)}.$$

Mean, SD, median, and range were reported. Bland–Altman analysis was performed to examine interocular and intersibling agreement. Sibling pairs with differences in DAF parameters in both eyes that exceeded the 95% limit of agreement were identified as a discordant family. An intersibling difference in BCVA of >10 letters was considered clinically significant. Absolute interocular and intersibling differences were compared for BCVA and DAF using the Mann–Whitney *U* test.

Results

Patients

We included 39 patients from 19 unrelated families with data on age at symptom onset (Table 1). One family had three siblings (F11) and the remaining families were all pairs with one set of twins (F16). A subset of these (32 siblings from 16 families) had age-matched BCVA and DAF areas (Table 2). Sixteen siblings from eight families had follow-up for comparison of age-matched DAF GR (Table 3).

Clinical Data

Thirty-seven patients had BCVA and DAF measurements. At baseline, the median age (range) was 39 (6–83) years (N = 37), and the median (range) disease duration was 15 years (5 years before onset to 65 years after onset, N = 35). Thirty patients had follow-up over a median (range) of 4.6 (0.5–8.7) years. Ten were mixed-sex, whereas nine were same-sex sibling pairings. Genotype Class A, B, and C was found in five, eight, and six families, respectively (Table 4).

Table 1. Baseline Demographics and Discordance in Age at Symptom Onset

Family No.	Genotype Class*	Patient No.	Year of Birth	Sex	Age at Symptom Onset (years)	Discordance in Symptom Onset (years)	Age at Baseline Examination (years)	Age at Final Examination (years)	Duration of Disease at Baseline (years)	Duration of Follow-Up (years)	Age-Matching during Follow up (Age of Siblings)
F1	B	P1	1983	M	17	1	29	36	12	7.04	Yes (29, 30)
		P2	1985	M	16		25	34	9	8.51	
F2	B	P3	1986	F	15	4	30	33	15	3.67	Yes (30, 30)
		P4	1988	M	19		24	31	5	7.21	
F3	A	P5	1977	F	10	3	39	41	29	2.67	Yes (38, 39)
		P6	1982	M	7		29	38	22	8.72	
F4	B	P7	1958	M	7	1	57	62	50	5.14	Yes, (58, 58)
		P8	1960	M	6		58	60	52	1.48	
F5	B	P9	1961	F	36	15	55	59	19	3.66	Yes (57, 57)
		P10	1959	M	51		57	61	6	4.51	
F6	A	P11	2001	M	9	2	12	19	4	6.25	Yes (12, 12)
		P12	2006	M	11		6	14	−5	3.16	
F7	A	P13	2003	M	7	1	15	18	8	2.53	Yes (18, 18)
		P14	1994	F	6		18	26	12	7.76	
F8	C	P15	1992	F	18	4	21	28	3	6.73	Yes (23, 23)
		P16	1990	F	22		23	29	1	6.24	
F9	C	P17	1958	M	62	35	58	62	−4	7.81	No
		P18	1967	F	27		48	53	21	5.27	
F10	B	P19	1937	M	22	14	75	79	53	3.55	Yes (75, 75)
		P20	1942	F	8		73	78	65	5.27	
F11	B	P21	1971	M	13	1, 3, 4	40	49	27	8.61	Yes (40, 41)
		P22	1977	M	12		41	—	29	—	
		P23	1969	F	16		—	—	—	—	
F12	A	P24	1963	F	9	3	53	57	44	4.79	No
		P25	1971	F	12		44	48	32	4.11	
F13	C	P26	1979	F	15	0	38	39	23	1.18	Yes (37, 38)
		P27	1982	F	15		35	37	20	1.18	
F14	A	P28	1993	F	8	1	27	28	19	0.51	Yes (26, 27)
		P29	1994	M	9		25	26	16	1.52	
F15	C	P30	1937	M	82	7	83	84	1	1.00	No
		P31	1942	F	75		75	78	0	3.16	
F16	B	P32	1990	F	NA	NA	30	—	—	—	Yes (30, 30)
		P33	1990	F	29		30	—	1	—	
F17	C	P34	1973	M	33	2	46	—	13	—	No
		P35	1978	F	31		42	—	11	—	
F18	B	P36	1971	F	NA	>32	48	49	—	1.53	No
		P37	1976	F	17		44	—	27	—	
F19	C	P38	1994	F	16	0	25	—	9	—	No
		P39	1987	F	16		—	—	—	—	

*Definition: Class A, severe biallelic mutations. Class B, an allele of intermediate severity in *trans* with a severe or intermediate allele. Class C, a mild allele in *trans* with a severe allele. NA, not applicable as patient remained asymptomatic at latest follow-up.

Table 2. Comparison of Age-Matched Sibling Pairs' Best Corrected Visual Acuity and Atrophy Area

Family No.	Genotype Class*	Patient No.	Sex	Age at Symptom Onset (years)	Age at Examination (years)	Duration of Disease at Match (years)	Age-Matched Measurements						Inter-sibling Differences						Foveal Sparing
							BCVA		DAF Area mm^2		DAF Radius, mm		BCVA		DAF Area, mm^2		DAF Radius, mm		
							Right	Left	Right	Left	Right	Left	Right	Left	Right	Left	Right	Left	
F1	B	P1	M	17	29	12	6	17	9.6	11.7	1.75	1.93	27	20	1.1	4.4	0.10	0.41	No
		P2	M	16	29	13	33	37	8.5	7.3	1.64	1.52							No
F2	B	P3	F	15	30	15	35	35	0.6	0.8	0.44	0.50	6	7	0.8	1.5	0.23	0.35	No
		P4	M	19	30	11	41	42	1.4	2.3	0.67	0.86							No
F3	A	P5	F	10	39	29	15	38	64.9	64.6	4.55	4.53	0	18	12.7	8.7	0.47	0.32	No
		P6	M	7	38	31	15	20	52.2	55.9	4.08	4.22							No
F4	B	P7	M	7	58	51	9	8	74.4	73.4	4.87	4.83	6	6	23.0	29.0	0.82	1.07	No
		P8	M	6	58	52	3	2	51.4	44.4	4.04	3.76							No
F5	B	P9	F	36	57	21	82	81	14.7	2.3	2.16	0.86	77	27	12.3	1.9	1.29	0.50	No
		P10	M	51	57	6	5	54	2.4	0.4	0.87	0.36							No
F6	A	P11	M	9	12	3	15	17	0.2	0.4	0.25	0.36	55	58	0.2	0.4	0.25	0.36	No
		P12	M	11	12	1	70	75	0.0	0.0	0.00	0.00							No
F7	A	P13	M	7	18	11	31	35	4.5	3.5	1.20	1.06	4	0	3.1	3.9	0.36	0.48	No
		P14	F	6	18	12	35	35	7.6	7.4	1.56	1.53							No
F8	C	P15	F	18	23	5	68	69	0.0	0.0	0.00	0.00	14	14	0.0	0.0	0.00	0.00	No
		P16	F	22	23	1	82	83	0.0	0.0	0.00	0.00							No
F10	B	P19	M	22	75	53	−30	−30	31.0	35.5	3.14	3.36	0	0	24.6	9.7	1.07	0.43	No
		P20	F	8	75	67	−30	−30	55.6	45.2	4.21	3.79							No
F11	B	P21	M	13	40	27	20	30	24.2	20.7	2.78	2.57	7	4	3.3	5.9	0.20	0.40	No
		P22	M	12	41	29	27	26	20.9	14.8	2.58	2.17							No
F13	C	P26	F	15	38	23	40	53	0.0	0.0	0.00	0.00	2	14	2.9	2.5	0.96	0.89	No
		P27	F	15	37	22	38	39	2.9	2.5	0.96	0.89							No
F14	A	P28	F	8	27	19	5	10	6.6	6.9	1.45	1.48	1	5	1.4	3.1	0.15	0.30	No
		P29	M	9	26	17	4	5	8.0	10.0	1.60	1.78							No
F16	B	P32	F	NA	30	NA	85	81	0.3	0.2	0.31	0.25	4	13	1.1	0.2	0.36	0.25	No
		P33	F	29	30	1	89	94	1.4	0.0	0.67	0.00							No

*Definition: Class A, severe biallelic mutations. Class B, an allele of intermediate severity in *trans* with a severe or intermediate allele. Class C, a mild allele in *trans* with a severe allele. DAF, dark autofluorescence; NA, not applicable as patient remained asymptomatic at latest follow-up.

Table 3. Comparison of Age-Matched Sibling Pairs' Atrophy Area and Effective Radius Growth Rates

Family No.	Genotype Class*	Patient No.	Sex	Age-Match (years)	Duration of Follow-Up (years)	Visual Acuity Change				Age-Matched Progression Rates in DAF				Inter-sibling Differences in DAF Growth			
						Baseline		Final		Area Growth Rate (mm^2/year)		Radius Growth Rate (mm/year)		Area Growth Rate (mm^2/year)		Radius Growth Rate (mm/year)	
						Right	Left	Right	Left	Right	Left	Right	Left	Right	Left	Right	Left
F1	B	P1	M	29	7.04	6	17	5	19	3.27	3.12	0.21	0.19	1.117	1.233	0.009	0.0004
		P2	M	29	8.51	23	30	20	31	2.15	1.89	0.22	0.19				
F2	B	P3	F	30	3.67	35	35	34	35	1.01	0.30	0.20	0.07	0.870	0.147	0.165	0.042
		P4	M	30	7.21	62	40	38	36	0.14	0.15	0.03	0.03				
F3	A	P5	F	39	2.67	15	38	12	31	0.45	1.73	0.02	0.06	0.273	0.442	0.013	0.031
		P6	M	38	8.72	15	20	15	20	0.72	2.17	0.03	0.09				
F4	B	P7	M	58	5.14	9	9	10	7	3.89	3.19	0.12	0.10	0.917	1.075	0.062	0.074
		P8	M	58	1.48	3	2	1	1	4.81	4.27	0.18	0.17				
F5	B	P9	F	57	3.66	86	86	80	82	2.02	1.34	0.15	0.23	0.467	0.006	0.043	0.008
		P10	M	57	4.51	56	81	−15	33	1.55	1.33	0.19	0.24				
F7	A	P13	M	18	2.53	42	63	31	35	0.36	0.04	0.05	0.01	0.176	0.205	0.032	0.018
		P14	F	18	7.76	35	35	29	33	0.18	0.24	0.02	0.02				
F10	B	P19	M	75	3.55	−30	−30	−30	−30	1.15	1.52	0.06	0.07	1.539	0.813	0.037	0.023
		P20	F	75	5.27	−30	−30	−30	−30	2.69	2.33	0.09	0.09				
F14	A	P28	F	27	0.51	5	10	10	11	1.17	3.12	0.13	0.32	0.677	1.011	0.078	0.111
		P29	M	26	1.52	7	7	4	5	1.85	2.11	0.20	0.21				

*Definition: Class A, severe biallelic mutations. Class B, an allele of intermediate severity in *trans* with a severe or intermediate allele.
DAF, dark autofluorescence.

Table 4. A Summary of Genetic Variants and Their Severities

Family No.	Patient No.	*ABCA4* Variants						Genotype Class†
		Allele 1	Protein	Severity	Allele 2	Protein	Severity	
F1	P1 P2	c.6079C>T	p.(Leu2027Phe)	Intermediate	c.768G>T	p.(Leu257Valfs*17)	Severe	B
F2	P3 P4	c.[2588G>C;5603A>T]	p.[Gly863Ala,Gly863del; Asn1868Ile]	mild[1] intermediate[2]	c.[5461–10T>C;5603A>T]	p.[Thr1821Valfs*13, Thr1821Aspfs*6]	Severe	B
F3	P5 P6	c.3617del	p.(Asn1206Metfs*3)	Severe	c.1496G>A	p.(Trp499*)	Severe	A
F4	P7 P8	c.4539+2028C>T	p.[=,Arg1514Leufs*36]	Intermediate	c.6031-6044delins18‡	p.(Ile2003Leufs*41)	Severe	B
F5	P9 P10	c.6079C>T	p.(Leu2027Phe)	Intermediate	c.4577C>T	p.(Thr1526Met)	Severe	B
F6	P11 P12	c.[5461–10T>C;5603A>T]	p.[,Thr1821Valfs*13, Thr1821Aspfs*6]	Severe	c.4320del	p.(Phe1440Leufs*6)	Severe	A
F7	P13 P14	c.4919G>A	p.(Val1617_Arg1640del, Arg1640Gln)	severe[3]	c.4919G>A	P.(Val1617_Arg1640del, Arg1640Gln)	severe[3]	A
F8	P15 P16	c.5691G>T	p.(Gln1897His)	Mild	c.768G>T	p.(Leu257Valfs*17)	Severe	C
F9	P17 P18	c.3113C>T	p.(Ala1038Val)	Mild intermediate[4]	c.2564G>A	p.(Trp855*)	Severe	C
F10	P19 P20	c.5537T>A	p.(Ile1846Asn)	Intermediate	c.[240_241del;5908C>T]	p.(Cys81Phefs*17)	Severe	B
F11	P21 P22 P23	c.6079C>T	p.(Leu2027Phe)	Intermediate	c.4577C>T	p.(Thr1526Met)	Severe	B
F12	P24 P25	c.3259G>A	p.(Glu1087Lys)	Severe	c.3190G>A	p.(Gly1064Ser)	Severe	A
F13	P26 P27	c.5882G>A	p.(Gly1961Glu)	Mild	c.4320del	p.(Phe1440Leufs*6)	Severe	C
F14	P28 P29	c.1574T>C	p.(Phe525Ser)	Severe	c.1906C>T	p.(Gln636*)	Severe	A
F15	P30 P31	c.5603A>T	p.(Asn1868Ile)	Mild	c.2894A>G	p.(Asn965Ser)	Severe	C
F16	P32 P33	c.1805G>A	p.(Arg602Gln)	Intermediate	c.4577C>T	p.(Thr1526Met)	Severe	B
F17	P34 P35	c.5882G>A	p.(Gly1961Glu)	Mild	c.4577C>T	p.(Thr1526Met)	Severe	C
F18	P36 P37	c.[2588G>C;5603A>T]	p.[Gly863Ala,Gly863del; Asn1868Ile]	Intermediate	c.634C>T	p.(Arg212Cys)	Intermediate	B
F19	P38 P39	c.6089G>A	p.(Arg2030Gln)	Mild	c.3407G>A	p.(Gly1136Glu)	Severe	C

†Definition: Class A, severe biallelic mutations. Class B, an allele of intermediate severity in trans with a severe or intermediate allele. Class C, a mild allele in trans with a severe allele.

‡c.6031_6044delinsAGTATTTAACCAATATTT.

References.

1. Sangermano, R., et al, ABCA4 midigenes reveal the full splice spectrum of all reported noncanonical splice site variants in Stargardt disease. Genome Res, 2018. 28(1): p. 100-110.

2. Fakin, A., et al, The Effect on Retinal Structure and Function of 15 Specific ABCA4 Mutations: A Detailed Examination of 82 Hemizygous Patients. Invest Ophthalmol Vis Sci, 2016. 57(14): p. 5963-5973.

3. Schulz, H.L., et al, Mutation Spectrum of the ABCA4 Gene in 335 Stargardt Disease Patients From a Multicenter German Cohort-Impact of Selected Deep Intronic Variants and Common SNPs. Invest Ophthalmol Vis Sci, 2017. 58(1): p. 394-403.

4. Garces, F., et al, Correlating the Expression and Functional Activity of ABCA4 Disease Variants With the Phenotype of Patients With Stargardt Disease. Invest Ophthalmol Vis Sci, 2018. 59(6): p. 2305-2315.

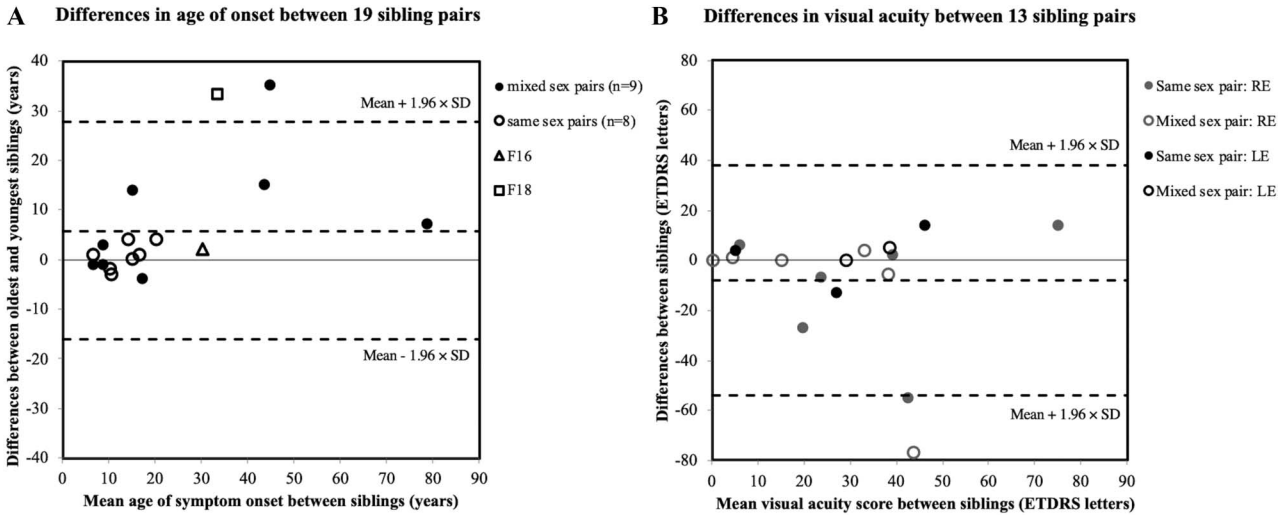

Fig. 1. Bland–Altman plots of differences in age at symptom onset across 19 families (**A**) and best-corrected visual acuity between 13 sibling pairs (**B**). The central dashed line represents the mean difference and the upper and lower dashed lines, calculated as mean ± 1.96 × SD, represent the upper and lower limits of agreement.

After excluding two asymptomatic patients (P32 aged 30 and P36 aged 49 years) from two families, the median (range) age at onset for the remaining 37 patients was 16 (6–82) years. The median (range) absolute difference in age at onset between sibling pairs was 3 (0–35) years. Five sibling pairs (F5, F9, F10, F15, F18) showed an intersibling discordance in age at onset of >5 years; namely, 15, 35, 14, seven, and >33 years, respectively (Figure 1). In four of these, the female sibling had an earlier onset. In the fifth discordant sibling pair, the younger of the two sisters had the earlier onset.

Thirteen sibling pairs had examinations that allowed for age-matched comparisons (Table 2); of which, 6 were mixed sex and seven were same-sex pairs. Median (range) absolute interocular asymmetry in BCVA was 1.5 (0–49) letters (see **Supplementary Table S1**, **Supplemental Digital Content 2**, http://links.lww.com/IAE/B682, and **Figure S2**, **Supplemental Digital Content 1**, http://links.lww.com/IAE/B684). Conversely, the median (range) absolute difference in age-matched BCVA was 6 (0–77) and 10 (0–58) letters in the right and left eyes, respectively. The overall absolute difference between siblings (both eyes) was greater than the absolute differences between eyes ($P = 0.01$). Four sibling pairs (F1, F5, F6, F8) had an age-matched intersibling difference in BCVA greater than 10 letters in both eyes; of which, one was a mixed-sex pair, where the male sibling had a worse BCVA. A Bland–Altman plot

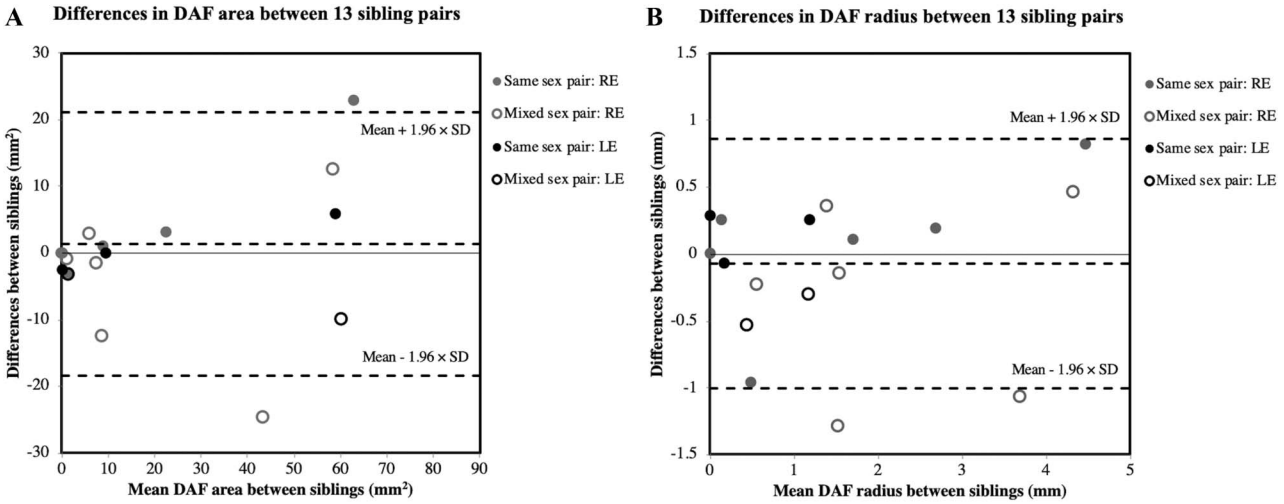

Fig. 2. Bland–Altman plots of differences in age-matched DAF area (**A**) and radius (**B**) in the right and left eyes between 13 sibling pairs. The central dashed line represents the mean difference and the upper and lower dashed lines, calculated as mean ± 1.96 × SD, represent the upper and lower limits of agreement.

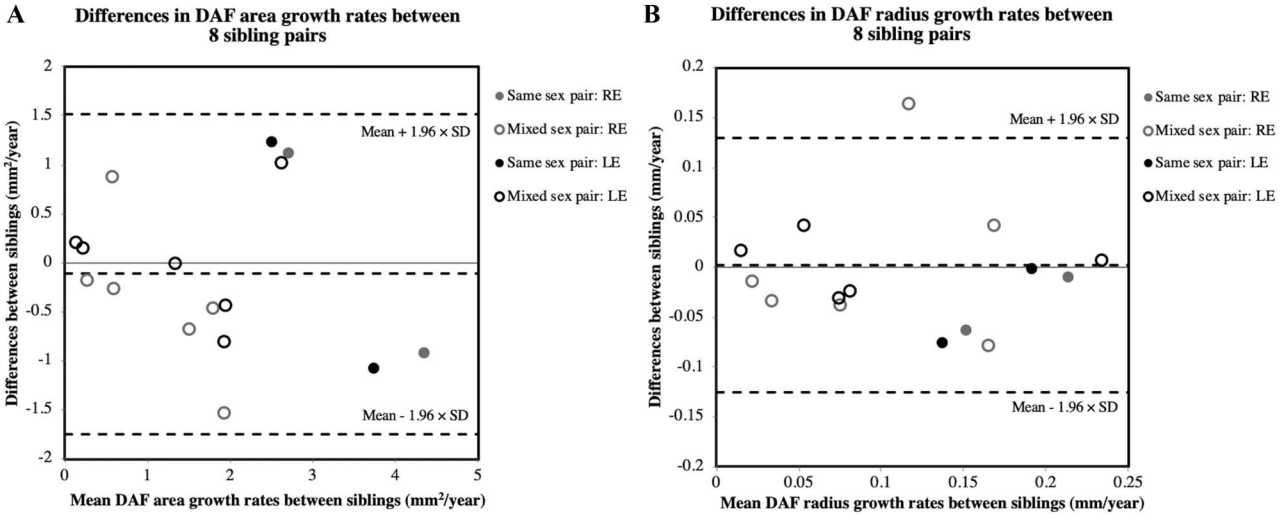

Fig. 3. Bland–Altman plots of differences in age-matched DAF area (**A**) and radius (**B**) growth rates for the right and left eyes between eight sibling pairs. The central dashed line represents the mean difference and the upper and lower dashed lines, calculated as mean ± 1.96 × SD, represent the upper and lower limits of agreement.

of the intersibling BCVA difference against the mean is shown in Figure 1.

Dark Autofluorescence

Four patients from three families did not have DAF identified in both eyes. Interocular asymmetry was greater with larger DAF lesions; however, this trend was eliminated by square root transformation (see **Supplementary Figures S3 and S4**, **Supplemental Digital Content 1**, http://links.lww.com/IAE/B684). The median (range) absolute interocular asymmetry in the DAF radius was 0.13 (0–1.31) mm. In contrast, the median (range) absolute intersibling difference in age-matched DAF radius was 0.36 (0–1.29) and 0.40 (0–1.07) mm in the right and left eyes, respectively. Overall absolute differences in intersibling DAF area and radius were greater than the absolute differences between eyes (P = 0.04 for area and P = 0.001 for radius). Three (F3, F4, F10) and two (F4, F13) sibling pairs had an age-matched discordance in DAF area and radius of greater than 7.55 mm^2 and 0.65 mm, respectively, in both eyes. Bland–Altman plots of intersibling DAF area and radius are shown in Figure 2.

Eight sibling pairs were examined for concordance in DAF GR at an age-matched time point (Table 3). The median (range) absolute interocular asymmetry in DAF area and radius GR was 0.36 (0.01–1.95) mm^2 per year and 0.024 (0.001–0.192) mm per year, respectively (see **Supplementary Figures S5 and S6**, **Supplemental Digital Content 1**, http://links.lww.com/IAE/B684). In contrast, the median (range) absolute intersibling difference in DAF area GR were 0.77 (0.18–1.54) and 0.63 (0.01–1.23) mm^2 per year in the right and left eyes, respectively. Similarly, the median (range) absolute intersibling difference in DAF radius GR was 0.040 (0.009–0.165) and 0.027 (0.000–0.111) mm per year in right and left eyes, respectively. The difference between absolute interocular and intersibling GR was not statistically significant (P = 0.44 for area GR and P = 0.61 for radius GR). Notably, one family (F2) had a difference in DAF radius GR greater than 0.13 mm per year (95% limits of interocular agreement) in one eye. Bland–Altman plots of intersibling DAF area and radial GR are shown in Figure 3.

Electrophysiology Concordance

Full-field ERG was performed on 33 patients of which 15 were sibling pairs (see **Supplementary Table S2**, **Supplemental Digital Content 3**, http://links.lww.com/IAE/B683). Five pairs had an age difference at the time of testing of > 10 years (mean = 21; range: 11–34 years). The remaining 10 sibling pairs had a mean age difference of 4.4 (range, 11–9.5) years. Concordance in electrophysiology groups among the 10 sibling pairs was 80%. Two discordant pairs had a younger sibling in Group 1 (macular involvement only) with the older sibling demonstrating additional cone dysfunction (F6) or cone–rod dysfunction (F16) at an older age, 3.5 (F6) and 3.7 (F16) years at the time of testing (Table 5). Both of these discordant pairs were tested on the same device (Roland Consult).

Illustrative Cases of Discordance in Phenotype

Two male siblings (F1) with a similar age at onset, carrying c.[6079C>T];[768G>T], had discordant BCVA with a difference of 27 (6 vs. 33) and 20 (17

Table 5. Electroretinography Characteristics of the Stargardt Disease Sibling Pairs

Family No.	Genotype Class*	ERG Group	ERG System†	Patient No.	Year of Birth	Age at Time of ERG (years)	Discordance in Age at ERG	PERG Abnormal	mfERG Abnormal	ffERG—Cone Dysfunction	ffERG—Rod Dysfunction	ERG Group
F1	B	3	LKC	P1	1983	28	11.1	—	Diffuse	Yes	Yes	3
		1	LKC	P2	1985	17		Yes	—	No	No	1
F2	B	3	RC	P3	1986	31	6.8	Yes	Foveal	Yes	Yes	3
		3	RC	P4	1988	24		No	Foveal	Yes	Yes	3
F3	A	3	RC	P5	1977	39	30.5	Yes	—	Yes	Yes	3
		3	In house	P6	1982	9		Yes	—	Yes	Yes	3
F5	B	3	RC	P9	1961	56	3.9	Yes	Parafoveal	Yes	Yes	3
		3	LKC	P10	1959	52		Yes	Parafoveal	Yes	Yes	3
F6	A	1	RC	P11	2001	11	3.5	Yes	—	No	No	1
		2	RC	P12	2006	15		No	Foveal	Yes	Yes	2
F7	A	3	RC	P13	2003	10	9.5	Yes	—	Yes	Yes	3
		3	RC	P14	1994	19		Yes	Diffuse	Yes	Yes	3
F8	C	1	RC	P15	1992	21	2.0	Yes	Foveal	No	No	1
		1	RC	P16	1990	23		No	Foveal	No	No	1
F9	C	3	RC	P17	1958	59	11.6	Yes	Parafoveal	Yes	Yes	3
		2	RC	P18	1967	48		Yes	—	Yes	No	2
F11	B	3	RC	P21	1971	47	34.1	Yes	—	Yes	Yes	3
		1	In house	P22	1977	13		Yes	—	No	No	1
F12	A	3	In house	P24	1963	26	4.4	—	—	Yes	Yes	3
		3	In house	P25	1971	22		—	—	Yes	Yes	3
F14	A	2	LKC	P28	1993	9	16.9	Yes	—	Yes	No	2
		3	RC	P29	1994	26		Yes	Diffuse	Yes	Yes	3
F15	C	2	RC	P30	1937	83	4.9	Yes	Diffuse	Yes	No	2
		1	RC	P31	1942	78		Yes	Parafoveal	No	No	1
F16	B	1	RC	P32	1990	26	3.7	No	Parafoveal	No	No	1
		2	RC	P33	1990	30		No	Parafoveal	Yes	Yes	3
F17	C	1	LKC	P34	1973	32	1.1	Yes	Foveal	No	No	1
		1	LKC	P35	1978	31		Yes	Foveal	No	No	1
F19	C	1	RC	P38	1994	20	4.3	No	Foveal	No	No	1
		1	LKC	P39	1987	16		Yes	—	No	No	1

*Definition: Class A, severe biallelic mutations. Class B, an allele of intermediate severity in *trans* with a severe or intermediate allele. Class C, a mild allele in *trans* with a severe allele.

†Definition: in-house device is a custom-built ERG instrument that used blue light for dim flash scotopic function assessment before 1999, LKC is the UTAS E-3000 system (LKC Technologies, Inc., Gaithersburg, USA) used between 1999 and 2012 and RC (Roland Consult) is the RETIPort 3.2 (Roland Consult, Brandenburg, Germany) used from 2012 onwards.

ffERG, full-field electroretinography; mfERG, multifocal electroretinography; PERG, pattern electroretinography.

Fig. 4. Ultra-widefield fundus autofluorescence images of the right and left eye of siblings from Family 1 (**A**) and Family 4 (**B**). In panel A, two male siblings from F1 with a similar age at symptom onset (17 and 16 years) and DAF area (9.6 vs. 8.5 mm^2 in the right eye and 11.7 vs. 7.3 mm^2 in the left eye) had a discordant age-matched BCVA (6 vs. 33 ETDRS letters in the right eye and 17 vs. 37 ETDRS letters in the left eye). In contrast, panel B shows two male siblings from F4 with a similar BCVA (9 vs. 3 ETDRS letters in the right eye and 8 vs. two ETDRS letters in the left eye) despite large differences in the age-matched DAF area (74.4 vs. 51.4 mm^2 in the right eye and 73.4 vs. 44.4 mm^2 in the left eye) and DAF radius (4.87 vs. 4.04 mm in the right eye and 4.83 vs. 3.76 mm in the left eye). ETDRS, Early Treatment Diabetic Retinopathy Study.

vs. 37) letters in right and left eyes, respectively, at the same age despite smaller differences in DAF area (9.6 vs. 8.5 and 11.7 vs. 7.3 mm^2 in the right and left eyes, respectively) (Figure 4A and Table 2). Interestingly, at 35 years of age, the right eye of both brothers showed evidence of a small residual central hyperAF island. However, the c.[6079C>T];[768G>T] variants have not been associated with foveal sparing. Furthermore, background stippled hyper/hypoAF was more extensive in the younger brother extending beyond the equator. In contrast, two male siblings from F4 both carrying c.[4539 + 2028C>T];[6031_6044delins18] showed no difference in BCVA (9 vs. 3 and 8 vs. 2 letters) despite large differences in the DAF area (74.4 vs. 51.4 and 73.4 vs. 44.4 mm^2 in the right and left eyes, respectively) (Figure 4B and Table 2). Widespread background stippled hypo/hyperAF was noted in both brothers, albeit P8 demonstrated greater peripapillary DAF extension.

A mixed-sex sibling pair from F5 carrying c.[6079C>T];[4577C>T] had a 15-year difference in their age at onset (36 vs. 51 years). Despite the late onset and smaller DAF area (2.4 vs. 14.7 and 0.4 vs. 2.3 mm^2 in the right and left eyes, respectively), the older brother had a reduced age-matched BCVA (5 vs. 82 and 54 vs. 81 letters in the right and left eyes, respectively) (Figure 5A). Another same-sex sibling pair from F11 with c.[6079C>T];[4577C>T] had a much earlier but concordant age at onset (13 and 12 years) and DAF area (24.2 vs. 20.9 and 20.7 vs. 14.8 mm^2 in the right and left eyes, respectively) (Figure 5B). Despite carrying identical biallelic *ABCA4* variants, at the age of 40 years, this same-sex sibling pair had more extensive DAF lesions than the mixed-sex sibling pair from F5 at age 57 years.

Another mixed-sex sibling pair from F10 carrying c.[240_241del;5908C>T];[5537T>A] had a discordance of 14 years in their age at onset (8 vs. 22 years). Although BCVA was hand motions in both siblings at 75 years, the DAF area was significantly greater in the female sibling (Figure 6A). However, the radius GR was similar. Large discordance in age at onset was also seen in the same-sex sibling pair from F18 carrying c.[2588G>C:5603A>T];[634C>T]. The younger sibling had an age at onset of 17 years, whereas the older sibling remained asymptomatic at 49 years with foveal sparing (Figure 6B).

Two mixed-sex siblings from F9 carrying c.[3113C>T];[2564G>A] had a discordant age at onset (27 vs. 62 years) (Figure 7A). The female sibling showed a significantly greater DAF area with no foveal sparing despite being 9 years younger at the time of imaging. Two mixed-sex siblings from F15 carrying c.[5603A>T];[2894A>G] also showed an earlier onset in the female sibling by 7 years (Figure 7B). The male sibling showed foveal sparing despite being 6 years older at the time of imaging. In contrast, the female sibling showed early foveal involvement despite a similar distribution of flecks.

Genotype Correlation

A total of 27 unique *ABCA4* alleles were identified, five of which were complex (Table 4). The most common variant was c.4577C>T (4 compound heterozygous families), followed by c.6079C>T (3 compound

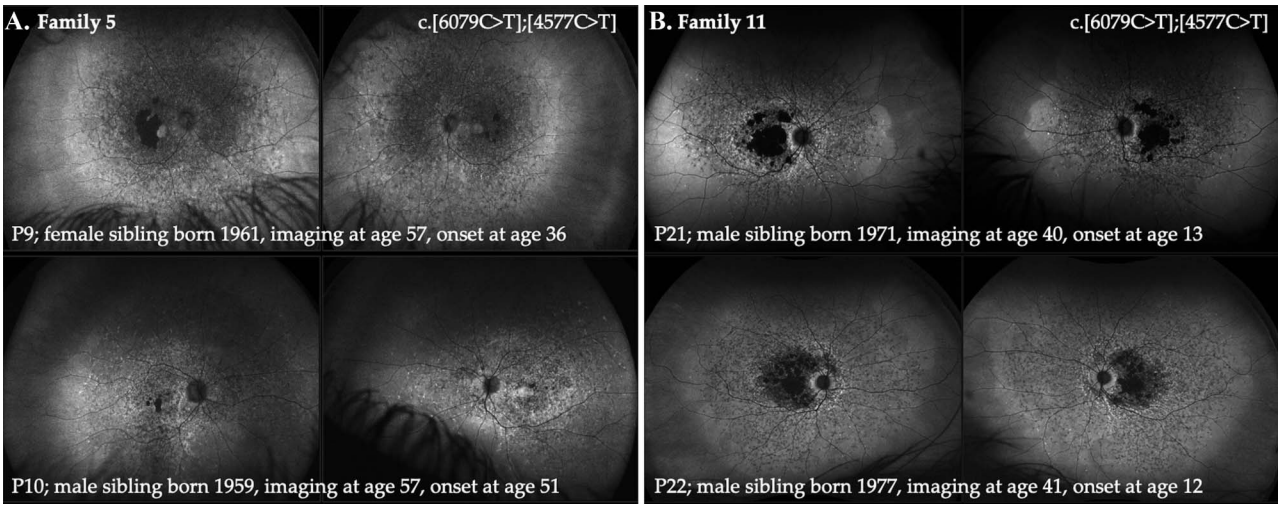

Fig. 5. Ultra-widefield fundus autofluorescence images of the right and left eyes of siblings from Family 5 (**A**) and Family 11 (**B**) harboring the same biallelic mutations c.[6079C>T];[4577C>T] with discordant intersibling best-corrected visual acuity (F5) (82 vs. five ETDRS letters in the right eye and 81 vs. 54 ETDRS letters in the left eye) and DAF area (F11) (24.2 vs. 20.9 mm^2 in the right eye and 20.7 vs. 14.8 mm^2 in the left eye). ETDRS, Early Treatment Diabetic Retinopathy Study.

heterozygous families). Five families had biallelic severe/nullizygous variants and their median (range) age at symptom onset was 9 (6–12) years with a mean discordance of 2 years. In contrast, the median (range) age at onset in those carrying a mild variant *in trans* with a severe variant was 24.5 (15–82) years with a mean discordance of 8 years.

Discussion

We compared phenotypes between siblings carrying identical *ABCA4* variants and found a discordant age at onset in five of 19 families (26%). An association with genotype Class B (3 of 8) or Class C (2 of 6), mixed-sex sibling pairing (4 of 10 mixed sex vs. 1 of 9 same sex) and an earlier onset in the female sibling suggest that sex may have a modifying effect. This could be attributed to earlier development of macular atrophy and foveal involvement in female patients. Lois et al[10] and Valkenburg et al[11] reported five of 15 families (33%) and 10 of 17 families (59%), respectively, with a discordant (>5 years difference) age at onset. Lois et al[10] found that four of eight mixed-sex sibling pairs and one of seven same-sex sibling pairs had a discordant age at onset. However, there was no genotyping to confirm identical *ABCA4* variants. In contrast, Valkenburg et al[11]

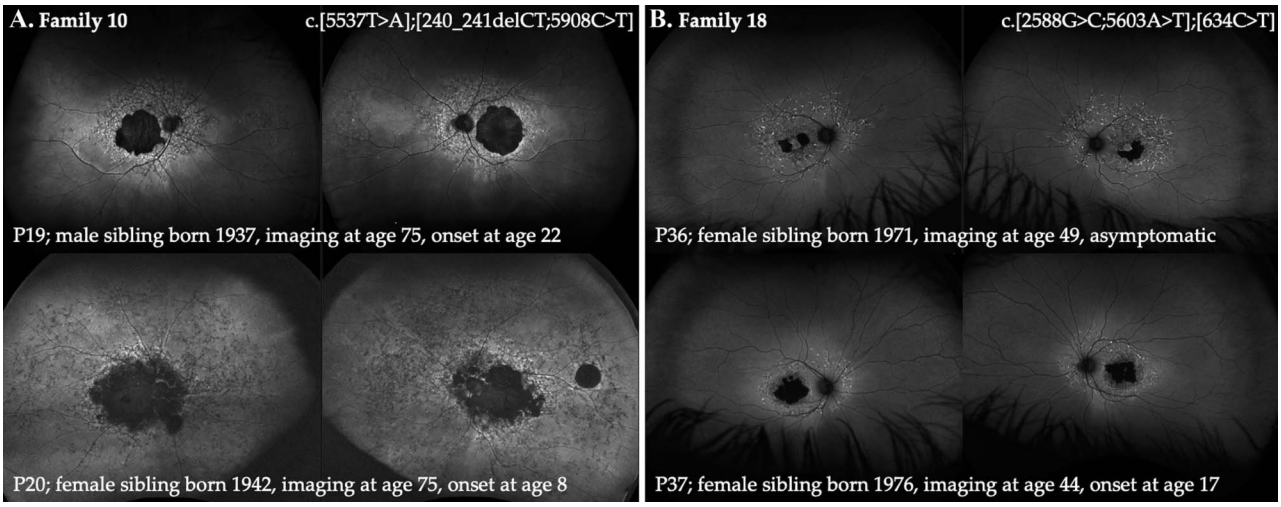

Fig. 6. Ultra-widefield fundus autofluorescence images of the right and left eyes of siblings from Family 10 (**A)** and Family 18 (**B)** showing a discordance in age at symptom onset with a difference of 14 and >32 years, respectively. In F10, BCVA was hand motions in both siblings at 75 years of age, although the DAF area was significantly greater in the female sibling [**A**] (55.6 vs. 31.0 mm^2 in the right eye and 45.2 vs. 35.5 mm^2 in the left eye).

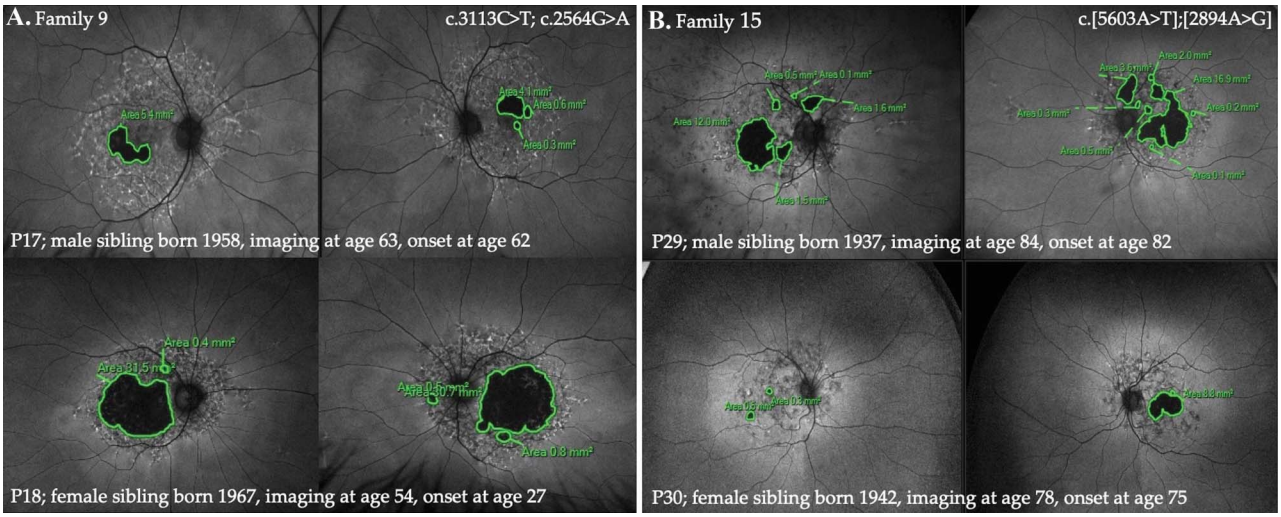

Fig. 7. Ultra-widefield fundus autofluorescence images of the right and left eyes in two discordant mixed sex sibling pairs. In Family 9, the female sibling showed a significantly greater area of DAF area (1.0 vs. 21 mm^2 in the right eye and 1.4 vs. 19.4 mm^2 in the left eye) despite being 9 years younger than her male counterpart at the time of imaging [**A**]. In Family 15, an earlier symptom onset in the female sibling (75 vs. 82 years) was noted as compared with her older brother by 7 years [**B**].

reported that two of five families with a Class A genotype had a discordant age at onset of 6 versus 14 years and 4 versus 10 years, respectively. However, the majority were found to have Class B (5 of 8) and Class C (3 of 4) genotypes. Similarly, Lois et al[10] found that six pairs had an earlier onset in the female sibling, but overall, there was no significant difference. Differences in penetrance between the sexes have been reported in patients carrying Class C variants: c.5603A>T and c.5882G>A. Runhart et al[28] reported a higher rate of penetrance in female patients carrying c.5603A>T or c.5882G>A variants (class C) and attributed this sex ratio imbalance to differences in sex hormones. They could not rule out potential environmental or other genetic modifier effects. Notably, they did not find a difference in the median age at onset between male and female patients carrying c.5603A>T (female patients at 40 years vs. male patients at 43 years) or c.5882G>A (female patients at 21.0 years and male patients at 19.5 years). We have previously shown that there is no abnormal AF signal beyond the affected fovea for those carrying c.5882G>A.[29] Given the current small sample sizes, larger genetically matched sibling cohorts are required to investigate discordance in age at onset.

We examined BCVA and DAF lesion size at an age-matched time point in 16 families. Previous studies have compared the BCVA at different ages between siblings[10] or standardized against disease duration.[11] Given that age at onset is subject to recall bias and is dependent on the extent of foveal involvement, we used age-matched measurements. As compared with absolute interocular asymmetry, we found a significant increase in the absolute intersibling difference for BCVA, DAF area, and radius. When each family was examined for variability that exceeded interocular limits of agreement, we found only two families (15%) with intersibling discordance in BCVA (F5 and F6), three families (23%) with discordance in DAF area (F3, F4, and F10), and two families (15%) with intersibling discordance in DAF radius (F4 and F13). The mismatch between BCVA and DAF intersibling discordance was explained by large, foveal sparing DAF lesions and the floor effect of BCVA when DAF area reaches a certain size. Valkenburg et al[11] reported differences in BCVA between 14 sibling pairs matched for disease duration and attributed this difference to a variable disease progression rate. They noted intersibling concordance of FAF patterns using the central 30° field. However, they only compared the DAF area between siblings in four families matched for disease duration and did not provide longitudinal data to support their hypothesis that discordant disease progression rate was the main driver of discordance in disease severity.

We examined eight sibling pairs' DAF area and radius GR at an age-matched time point. Compared with interocular asymmetry in GR, we did not find a significant difference in intersibling discordance because no families had intersibling discordance in GR that exceeded the 95% interocular limits of agreement in both eyes. Therefore, despite asymmetry in disease severity at an age-matched time point, there was no significant difference between siblings in with respect to their DAF area and radius GR. Greater

variability in disease severity as compared with DAF progression raises the possibility that the processes that lead to the formation of atrophy are more susceptible to genetic and environmental modifiers, whereas the growth of DAF lesions has a natural history that is mostly dependent on the baseline DAF area[30,31] and genotype.[12,32–34] Fakin et al[35] described genotype-dependent FAF progression in 19 STGD1 patients using the $30° \times 30°$ frame whereby the area of reduced AF was shown to increase by 1.5, 1.2, and 0.03 mm^2 per year in those harboring biallelic null mutations, a splice mutation in *trans* with a null mutation or c.5882G>A in *trans* with a null mutation. Fakin et al[36] has characterized the degree of retinal dysfunction conferred by 15 specific *ABCA4* variants using electroretinography (ERG) responses. We compared electrophysiology tracings between sibling pairs and found a discordant ERG group in two of 15 families (20%); of which, the older sibling in these pairs demonstrating additional cone (F6) or cone–rod (F16) dysfunction. This is interesting considering that Fujinami et al[18] showed that ERG assessment at different time points may be of limited significance because of low rates of conversion between ERG groups. Further sibling studies incorporating ERG comparisons and longitudinal changes are required to determine whether intersibling discordance exists for functional outcomes.

We observed intersibling concordance [F5] and discordance [F15, F18] with respect to foveal sparing. In our cohort, only two siblings from F19 were found to harbor the *ABCA4* variant c.6089G>A; of whom, only one had clinical data. Fujinami et al[37] reported a higher prevalence of the c.6089G>A variant in the foveal sparing group (6.45% vs. 1.07%). Singh et al[38] reported longitudinal follow-up of two sisters with a discordant phenotype; of which, one sister illustrated foveal atrophy with a homogenous background and the other sister demonstrated perifoveal macular atrophy with a heterogenous background. Importantly, one sibling was found to harbor an additional allele p.(Arg881Cys) and the second mutation in the other sibling was not identified.

Our study was limited by its small sample size and retrospective nature. There were significantly lower numbers of follow-up data for some siblings that limited the investigation of lesion GR between mixed-sex sibling pairs. There may have been bias in the clinical ascertainment of younger siblings with access to proactive screening following a STGD1 diagnosis of their older sibling. We attempted to match for age at examination in a substantial number of families. The DAF area measured using the image scale was not adjusted for axial length and may have led to minor measurement errors. A strength of our paper is that we have only included siblings pairs with identical ABCA4 variants by excluding families with siblings who have discordant variants. This contrasts with the report by Michaelides et al.[39] which illustrated phenotype concordance between sibling pairs with discordant ABCA4 variants.

Mixed-sex sibling pairs as well as those harboring Class B or Class C genotypes were more likely to show significant discordance in their age at onset with earlier symptoms observed in female siblings as compared with their male counterparts. After adjusting for age at examination, there was a significant sibling discordance in BCVA and DAF area beyond the expected limits of interocular asymmetry. The lack of significant intersibling differences in lesion growth rate warrants further investigation.

Key words: inherited retinal disease, retinal dystrophy, macular dystrophy, retinal imaging, ABCA4-associated retinopathy, clinical trial end point.

Acknowledgments

The authors thank Amanda Scurry and Jayme Glynn for their assistance in organizing the patient appointments and Maryam Saadat for performing retinal imaging. The AIRDR acknowledges the assistance of Enid Chelva, Ling Hoffman and Isabella Urwin from the Department of Medical Technology and Physics at the Sir Charles Gairdner Hospital.

References

1. Michaelides M, Hunt DM, Moore AT. The genetics of inherited macular dystrophies. J Med Genet 2003;40:641–650.
2. Fujinami K, Zernant J, Chana RK, et al. Clinical and molecular characteristics of childhood-onset Stargardt disease. Ophthalmol 2015;122:326–334.
3. De Roach JN, McLaren TL, Thompson JA, et al. The Australian inherited retinal disease Registry and DNA bank. Tasman Med J 2020;2:60–67.
4. Westeneng-van Haaften SC, Boon CJ, Cremers FP, et al. Clinical and genetic characteristics of late-onset Stargardt's disease. Ophthalmol 2012;119:1199–1210.
5. Heath Jeffery RC, Mukhtar SA, McAllister IL, et al. Inherited retinal diseases are the most common cause of blindness in the working-age population in Australia. Ophthalmic Genet 2021;42(4):431–439.
6. Burke TR, Tsang SH, Zernant J, et al. Familial discordance in Stargardt disease. Mol Vis 2012;18:227–233.
7. Huckfeldt RM, East JS, Stone EM, Sohn EH. Phenotypic variation in a family with pseudodominant Stargardt disease. JAMA Ophthalmol 2016;134:580–583.
8. Huang D, Thompson JA, Charng J, et al. Phenotype-genotype correlations in a pseudodominant Stargardt disease pedigree due to a novel ABCA4 deletion-insertion variant causing a splicing defect. Mol Genet Genomic Med 2020;8:e1259.
9. Aaberg TM. Stargardt's disease and fundus flavimaculatus: evaluation of morphologic progression and intrafamilial coexistence. Trans Am Ophthalmol Soc 1986;84:453–487.

10. Lois N, Holder GE, Fitzke FW, et al. Intrafamilial variation of phenotype in Stargardt macular dystrophy-Fundus flavimaculatus. Invest Ophthalmol Vis Sci 1999;40:2668–2675.
11. Valkenburg D, Runhart EH, Bax NM, et al. Highly variable disease courses in siblings with Stargardt disease. Ophthalmology 2019;126:1712–1721.
12. Heath Jeffery RC, Thompson JA, Lo J, et al. Atrophy expansion rates in Stargardt disease using ultra-widefield fundus autofluorescence. Ophthalmol Sci 2021;1:100005.
13. Marmor MF, Arden GB, Nilsson SE, Zrenner E. Standard for clinical electroretinography. Arch Ophthalmol 1989;107:816–819.
14. McCulloch DL, Marmor MF, Brigell MG, et al. ISCEV standard for full-field clinical electroretinography (2015 update). Doc Ophthalmol 2015;130:1–12.
15. Bach M, Brigell MG, Hawlina M, et al. ISCEV standard for clinical pattern electroretinography (PERG): 2012 update. Doc Ophthalmol 2013;126:1–7.
16. Hood DC, Bach M, Brigell M, et al. ISCEV standard for clinical multifocal electroretinography (mfERG) (2011 edition). Doc Ophthalmol 2012;124:1–13.
17. Lois N, Holder GE, Bunce C, et al. Phenotypic subtypes of Stargardt macular dystrophy-fundus flavimaculatus. Arch Ophthalmol 2001;119:359–369.
18. Fujinami K, Lois N, Davidson AE, et al. A longitudinal study of Stargardt disease: clinical and electrophysiological assessment, progression and genotype correlations. Am J Ophthalmol 2013;155:1075–1088.
19. De Roach JN, McLaren TL, Paterson RL, et al. Establishment and evolution of the Australian inherited retinal disease register and DNA bank. Clin Exp Ophthalmol 2013;41:476–483.
20. Chiang JP, Lamey T, McLaren T, et al. Progress and prospects of next-generation sequencing testing for inherited retinal dystrophy. Expert Rev Mol Diagn 2015;15:1269–1275.
21. den Dunnen JT, Dalgleish R, Maglott DR, et al. HGVS recommendations for the description of sequence variants: 2016 update. Hum Mutat 2016;37:564–569.
22. Thompson JA, De Roach JN, McLaren TL, et al. The genetic profile of Leber congenital amaurosis in an Australian cohort. Mol Genet Genomic Med 2017;5:652–667.
23. Richards S, Nazneen A, Bale S, et al. Standards and guidelines for the interpretation of sequence variants: a joint consensus recommendation of the American College of medical genetics and Genomics and the association for molecular pathology. Genet Med 2015;17:405–424.
24. Jarvik GP, Browning BL. Consideration of cosegregation in the pathogenicity classification of genomic variants. Am J Hum Genet 2016;98:1077–1081.
25. Schulze-Bonsel K, Feltgen N, Curau H, et al. Visual acuities "hand motion" and "counting fingers" can be quantified with the Freiburg visual acuity test. Invest Ophthalmol Vis Sci 2006;47:1236–1240.
26. Lange C, Feltgen N, Junker B, et al. Resolving the clinical acuity categories "hand motion" and "count fingers" using the Freiburg visual acuity test (FrACT). Graefes Arch Clin Exp Ophthalmol 2009;247:137–142.
27. Shen LL, Sun M, Grossetta Nardini HK, Del Priore LV. Natural history of autosomal recessive Stargardt disease in untreated eyes: a systematic review and meta-analysis of study and individual level data. Ophthalmology 2019;126:1288–1296.
28. Runhart EH, Khan M, Cornelis SS, et al. Association of sex with frequent and mild ABCA4 alleles in Stargardt disease. JAMA Ophthalmol 2020;138:1035–1042.
29. Heath Jeffery RC, Thompson JA, Lamey TM, et al. Classifying ABCA4 mutation severity using age-dependant ultra-widefield fundas autofluorescence-derived total lesion size. Retina 2021;41(12):2578–2588.
30. Muller PL, Pfau M, Treis T, et al. Progression of ABCA4-related retinopathy: prognostic value of demographic, functional, genetic, and imaging parameters. Retina 2020;40:2343–2356.
31. Heath Jeffery RC, Chen FC. Stargardt disease: multimodal imaging: a review. Clin Exp Ophthalmol 2021;49:498–515.
32. Georgiou M, Kane T, Tanna P, et al. Prospective cohort study of childhood-onset Stargardt disease: fundus autofluorescence imaging, progression, comparison with adult-onset disease, and disease symmetry. Am J Ophthalmol 2020;211:159–175.
33. Fujinami K, Lois N, Mukherjee R, et al. A longitudinal study of Stargardt disease: quantitative assessment of fundus autofluorescence, progression, and genotype correlations. Invest Ophthalmol Vis Sci 2013;54:8181–8190.
34. Di Iorio V, Orrico A, Esposito G, et al. Association between genotype and disease progression in Italian Stargardt patients: a retrospective natural history study. Retina 2019;39:1399–1409.
35. Fakin A, Robson AG, Fujinami K, et al. Phenotype and progression of retinal degeneration associated with nullizigosity of ABCA4. IOVS 2016;57:4668–4678.
36. Fakin A, Robson AG, Chiang JP, et al. The effect on retinal structure and function of 15 specific ABCA4 mutations: a detailed examination of 82 hemizygous patients. IOVS 2016;57:5963–5973.
37. Fujinami K, Sergouniotis PI, Davidson AE, et al. Clinical and molecular analysis of Stargardt disease with preserved foveal structure and function. Am J Ophthalmol 2013;156:487–501.e1.
38. Singh R, Fujinami K, Chen LL, et al. Longitudinal follow-up of siblings with a discordant Stargardt disease phenotype. Acta Ophthalmol 2014;92:e331–2.
39. Michaelides M, Chen LL, Brantley MA, et al. ABCA4 mutations and discordant ABCA4 alleles in patients and siblings with bull's-eye maculopathy. Br J Ophthalmol 2007;91:1650–1655.